Vortex stretching in a homogeneous isotropic turbulence

M Hirota, Y Nishio, S Izawa and Y Fukunishi

Mechanical Systems and Design, Graduate School of Engineering, Tohoku University, 6-6-01 Aramaki-Aoba, Aoba-ku, Sendai, Miyagi, 980-8579, Japan

E-mail: masato.hirota.r7@dc.tohoku.ac.jp

Abstract. Stretching vortices whose sizes are in the inertial subrange of a homogeneous isotropic turbulence are picked up, and the geometric relations with the neighboring vortices whose scales are twice larger are studied. Hierarchical vortices are extracted using a Fourier band-pass filter, and each extracted vortex is reconstructed as a set of short cylindrical segments along the vortex axis to discuss the vortex interactions. As a result, it is shown that the directions of larger vortices near the segments of the fast stretching vortices tend to be orthogonal to the direction of the stretching segments, and the locations of the larger vortices that contribute most to the stretching of smaller vortex segments are likely to be found in the direction with the relative angle of 45° from the axes of the stretching vortex segments. And, the vortices with the second highest contributions tend to be in the directions 45° from the stretching segments' axes and orthogonal to the directions of the highest contributing vortices.

1. Introduction

Turbulent flows consist of vortices of various scales interacting with each other. Energy is continuously transported from energy-containing vortices of larger scale to energy-dissipative vortices of smaller scale. This process is well known as the energy cascade of turbulence. Kolmogorov[1] theoretically derived that the energy flux in the inertial subrange was constant, and the slope of the energy spectrum was universally $-5/3$. This $-5/3$ energy spectrum has been confirmed by many experiments[2] and direct numerical simulations (DNS)[3]; however, the physical mechanism behind the theory is less understood.

Statistical properties of turbulent flows such as the energy cascade are believed to be due to the mutual interactions of hierarchical vortices, which occur locally and intermittently. In other words, local vortex behaviors, e.g. vortex formation, stretching and breaking down, should be responsible for the turbulent motions. For example, in free shear flows, primary vortices are firstly generated by the Kelvin-Helmholtz instability, and then, the secondary vortices, named rib vortices, develop between them in the streamwise direction. These secondary vortices are soon stretched owing to the strong shear generated by the primary vortices. As a result, three-dimensional deformation of the primary vortices takes place, and vortical structures become complicated[4]. Similar phenomena can be found in turbulent flows, in a fractal manner. Goto[5, 6] reported that the energy cascade in the inertial subrange is caused by the creation of smaller-scale vortex tubes in straining regions which can be found around the larger-scale vortex tubes. There is little doubt that vortex stretching is an important factor in the energy cascade process of turbulent flows.

In our previous studies[7], it has already been found that the vortices of a certain scale in the inertial subrange were likely to be stretched by vortices whose scales were twice larger. Leung *et al.*[8] also reported that vortices of a certain scale were predominantly stretched by the strain field of larger vortices whose scale was larger or comparable. The present study focuses on the stretching mechanism of vortices in a homogeneous isotropic turbulence. The relative positional relationships between a stretching vortex and twice larger vortices around it are investigated in detail.

2. Numerical method

The target is a homogeneous isotropic turbulence in a periodic box of 2π on a side, which is obtained by DNS. The three-dimensional vorticity transport equation is solved by a pseudo-spectral method. Total grid number is 512^3. Aliasing errors are completely removed by the phase shift method. Time integration is performed by a fourth-order classical Runge-Kutta method. In order to keep the flow field in a statistically equilibrium state, a solenoidal external force is randomly given to the low wavenumber region $1 \leq k \leq 2$, where k denotes a wavenumber. Figure 1 shows the energy spectrum of the flow field. The Taylor micro-scale Reynolds number Re_λ of the flow field is $Re_\lambda = 267$.

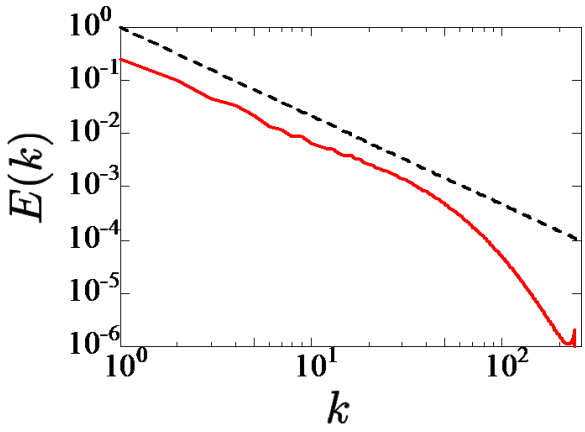

Figure 1. Energy spectrum of turbulent field: ——, present DNS data; - - - -, slope $\propto k^{-5/3}$.

3. Analysis procedures

3.1. Extraction and identification of multi-scale vortices

Vorticity fields of two different scales are extracted by Fourier band-pass filters with the center wavenumbers $k_c = 12\sqrt{2}$ and $6\sqrt{2}$, where the bandwidths are $k_c/\sqrt{2} \leq \boldsymbol{k} < \sqrt{2}k_c$. Vortical structures in the extracted vorticity fields are identified using the Q criterion. Regions where the Q value exceeds 75% of r.m.s. of the enstrophy density $\Omega_{\rm rms}$ are regarded as inside the vortices. Figure 2 shows the vortical structures before and after the filtering. Many tiny vortices are observed in the target turbulent field.

In order to discuss the geometric relation of these extracted vortices, each vortex is reconstructed as a set of cylindrical elements (vortex segments) by the following procedure:

(i) Compute the eigenvalues and the eigenvectors of the Hessian of Q at each computational grid point and determine the vortex axis as a line which connects the local maximum values of Q.

(ii) Place vortex segments which are grid width long along the vortex axes.

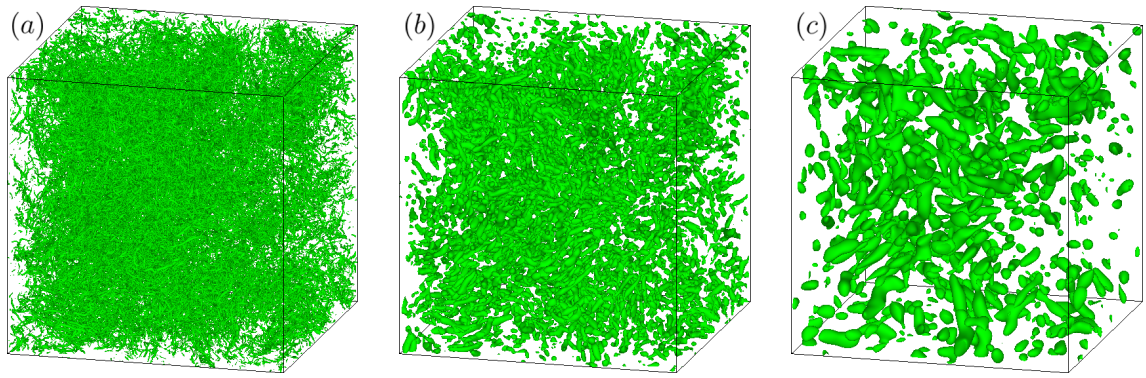

Figure 2. Turbulent vortical structures: (a) original vorticity field; (b) extracted at target scale $k_1 = 12\sqrt{2}$; (c) extracted at the scale twice larger $k_2 = 6\sqrt{2}$. Isosurface of $Q = 0.75\Omega_{\rm rms}$ is shown.

(iii) By applying the wavelet transformation to the vorticity distribution in the plane normal to each axis, estimate the radius of each segment as the most correlated scale of the wavelet coefficient.

(iv) Regard short vortices whose aspect ratios are less than one as noise and eliminate them.

(v) Determine the circulation of each segment so that each reconstructed vortex has the same circulation as that of the vortex region identified by the Q criterion.

By the procedure shown above, the vortical structures of scale $k_1 = 12\sqrt{2}$ and $k_2 = 6\sqrt{2}$ are reconstructed as a set of connected vortex segments. Thus, the velocity at any positions, induced by any vortex, can be estimated by applying the Biot-Savart law.

3.2. Geometric relations between fast-stretching vortex segments and their surrounding vortices
The stretching of a vortex segment of scale k_1 caused by larger vortices of scale k_2 is evaluated by the stretching speed γ, which is,

$$\gamma = \frac{1}{l_{\rm s}}\frac{dl_{\rm s}}{dt} = \frac{du_{\rm s}}{de_{\rm s}}, \tag{1}$$

where, $l_{\rm s}$ is the length of the vortex segment, and $u_{\rm s}$ is the velocity in the vortex axis $e_{\rm s}$ direction.

Fast stretching vortex segments whose stretching speeds are within top 10% of the whole vortex segments of scale k_1 are picked up, and the geometric relations between these fast stretching segments and their surrounding larger vortices of scale k_2 are investigated using the following procedure:

(i) Choose a fast stretching vortex segment of scale k_1 as the target segment.

(ii) Find vortices of scale k_2 in the vicinity of the target segment within $6R$, where R denotes the radius of the vortex segment of scale k_2.

(iii) Calculate the amount each vortex of scale k_2 stretches the target segment.

(iv) Find the vortex of scale k_2 with the highest contribution to stretching, referred as "No.1", and the vortex of the second highest contribution to stretching, referred as "No.2".

(v) Calculate stretching speeds γ' of the target segment caused by each vortex segment of the No.1 and No.2 vortices.

(vi) Average the radius $R_{\rm s}$, the position $\boldsymbol{x}_{\rm s}$ and the direction $\boldsymbol{e}_{\rm s}$ of the segments of the No.1 vortex, and then the No.2 vortex, using equations below.

$$R_{\rm s} = \sum_{i=1}^{n} \gamma_i' R_{{\rm s}i} \Big/ \sum_{i=1}^{n} \gamma_i', \tag{2}$$

$$\boldsymbol{x}_{\rm s} = \sum_{i=1}^{n} \gamma_i' \boldsymbol{x}_{{\rm s}i} \Big/ \sum_{i=1}^{n} \gamma_i', \tag{3}$$

$$\boldsymbol{e}_{\rm s} = \sum_{i=1}^{n} \gamma_i' \boldsymbol{e}_{{\rm s}i} \Big/ \sum_{i=1}^{n} \gamma_i', \tag{4}$$

where, i denotes the vortex segment number, and n is the total number of segments for each vortex.

(vii) Measure the averaged values of the relative position and the relative angle between the target segment and the No.1 vortex, and then the No.2 vortex.

(viii) Repeat the above procedure for all the fast stretching segments of scale k_1.

4. Results and discussion

Figure 3 shows the probability density function (PDF) of the cosine of an angle between the segment of the fast stretching vortex of scale $k_1 = 12\sqrt{2}$ and the top two vortices of scale $k_2 = 6\sqrt{2}$ that contribute to the stretching. The value of the PDF becomes higher where the cosine value is zero. This result means that the two contribution vortices of the larger scale tend to be orthogonal to a fast stretching vortex segment of the smaller scale. Figure 4 shows the joint probability density function of the relative positions of the No.1 vortices of scale k_2. The centers of the target vortex segments of scale k_1 are placed at the origin. The axes ξ and η correspond to the direction of the target vortex segments and its orthogonal direction. These axes are normalized by the averaged radius R of the No.1 vortices. The joint PDF becomes higher at the region where the relative angle is $\pm 45^\circ$ and where the distance is between R and $2R$. Figure 5 shows the joint PDF of the positions of the No.2 vortices. Again, the origin is the center of the target vortex segment. The axis Ξ is the direction of the No.1 vortices, and the axis H is orthogonal to Ξ. The No.2 vortices tend to appear $1.5R - 2.5R$ away from the target segments and in the direction orthogonal to the direction of the No.1 vortices.

These results indicate that the vortex stretching is likely to be caused under the specific configuration of surrounding vortices, not just randomly distributed vortices.

5. Conclusions

Geometric relations between two different scale vortices were investigated by focusing on the vortex stretching. It was found that the segments of fast stretching vortices tended to be orthogonal to the directions of vortices whose scales were twice larger. Besides, the vortices of the highest contributions to the stretching were likely to be found in the directions with the relative angle of 45° to the axes of the stretching vortex segments, and the vortices of the second highest contributions tended to appear also in directions 45° from the stretching segments and orthogonal to the directions of the vortices of the highest contributions.

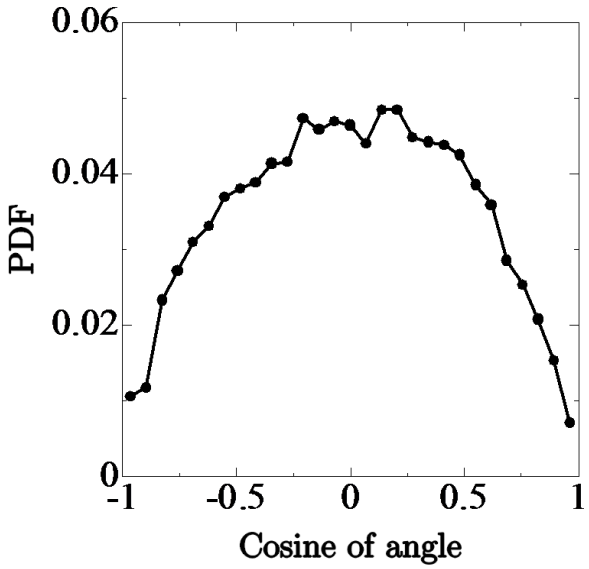

Figure 3. PDF of the cosine of an angle between the segment of the fast stretching vortex of scale $k_1 = 12\sqrt{2}$ and the vortices with the highest contributions to the stretching (No.1) and the second highest contributions (No.2).

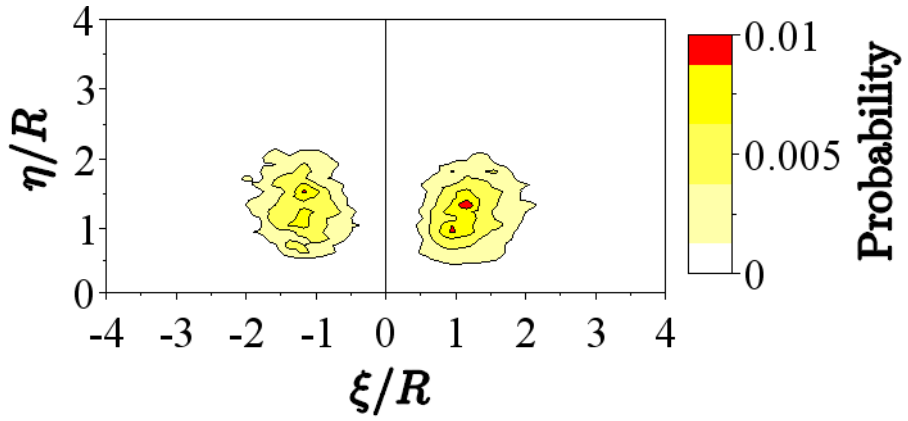

Figure 4. Joint PDF of positions of vortices with the highest contributions to the stretching (No.1) relative to the fast stretching vortex segments of scale k_1, where ξ denotes the axes of segments of scale k_1.

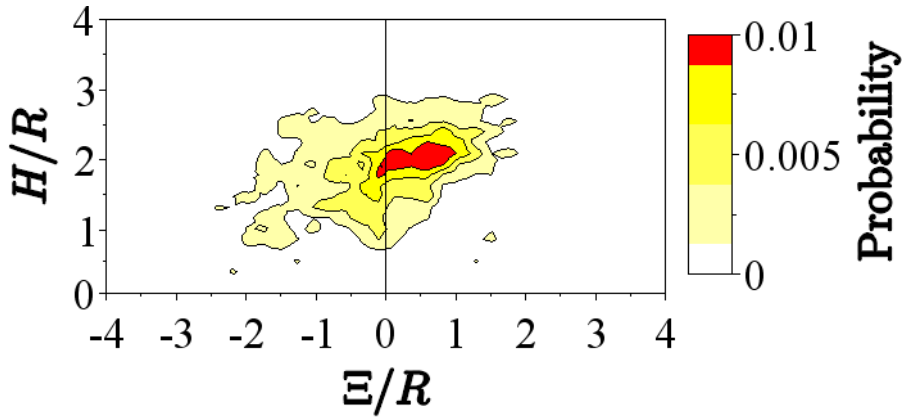

Figure 5. Joint PDF of the positions of vortices with the second highest contributions to the stretching (No.2) relative to the fast stretching segments of scale k_1, where Ξ denotes the direction of the No.1 vortices of scale k_2.

References

[1] Kolmogorov A N 1941 *Dokl. Akad. Nauk SSSR* **30** 301–305
[2] Tsuji Y 2009 *Fluid Dynamics Research* **41** 064003
[3] Ishihara T, Gotoh T and Kaneda Y 2009 *Annu. Rev. Fluid Mech.* **41** 165–180
[4] Lasheras J C and Choi H 1988 *J. Fluid Mech.* **189** 53–86
[5] Goto S 2008 *J. Fluid Mech.* **605** 355–366
[6] Goto S 2012 *Prog. Theor. Phys. Suppl.* **195** 139–156
[7] Hirota M, Shigeta M, Izawa S and Fukunishi Y 2013 *Proc. 27th Symp. Computational Fluid Dynamics* A02-1 (in Japanese)
[8] Leung T, Swaminathan N and Davidson P A 2012 *J. Fluid Mech.* **710** 453–481